Korean Journal of Remote Sensing, Vol.21, No.5, 2005, pp.405~415

Detection of Microphytobenthos in the Saemangeum Tidal Flat by Linear Spectral Unmixing Method

Yoon-Kyung Lee*, Joo-Hyung Ryu, and Joong-Sun Won* †**

Department of Earth System Sciences, Yonsei University*

Ocean Satellite Research Group, Korea Ocean Research & Development Institute**

Abstract : It is difficult to classify tidal flat surface that is composed of a mixture of mud, sand, water and microphytobenthos. We used a Linear Spectral Unmixing (LSU) method for effectively classifying the tidal flat surface characteristics within a pixel. This study aims at 1) detecting algal mat using LSU in the Saemangeum tidal flats, 2) determining a suitable end-member selection method in tidal flats, and 3) find out a habitual characteristics of algal mat. Two types of end-member were built; one is a reference end-member derived from field spectrometer measurements and the other image end-member. A field spectrometer was used to measure spectral reflectance, and a spectral library was accomplished by shape difference of spectra, r.m.s. difference of spectra, continuum removal and Mann-Whitney U-test. Reference end-members were extracted from the spectral library. Image end-members were obtained by applying Principle Component Analysis (PCA) to an image. The LSU method was effective to detect microphytobenthos, and successfully classified the intertidal zone into algal mat, sediment, and water body components. The reference end-member was slightly more effective than the image end-member for the classification. Fine grained upper tidal flat is generally considered as a rich habitat for algal mat. We also identified unusual microphytobenthos that inhabited coarse grained lower tidal flats.

Key Words : Linear spectral unmixing, Saemangeum tidal flat, microphytobenthos, spectral library, Landsat.

1. Introduction

Tidal current, fresh water from landward and fluctuated salinity provide tidal flats a unique environment that is distinguished from other ecosystems. Microphytobenthos are principal primary producers that supply nutrients to the intertidal ecosystem (Koh, 2001). It is called algal mat that microphytobenthos are in full bloom to make a patch when temperature and nutritive salts are in the most suitable for their growing. Algal mat not only provide nutrients but also build extracellular polymeric substance network which prevent erosion of sediments. It is important to monitor the distribution and density of algal mat for evaluating primary production in a tidal flat, its effect to the intertidal ecosystem and sediment stability (Paterson *et al.*, 1998; Riethmuller *et al.*, 2000).

Received 14 September 2005; Accepted 25 October 2005.

† Corresponding Author: J. – S. Won (jswon@yonsei.ac.kr)

The traditional hard classification methods, inferring a key characteristic of surface covers, are hard to define correlation between remote sensed data and field data because one pixel of remote sensed data with a large spatial resolution is rarely covered with a homogeneous substance on the ground. Spectral unmixing is one of soft classification methods that defines the surface covers to sub-pixels according to the surface abundances. Especially, linear spectral unmixing (LSU) assumes that each pixel consists of mixtures of each spectra which react each photon in the field of view (FOV) (Roberts *et al.*, 1998).

Microphytobenthos in Korean tidal flats usually bloom from January to March. Fine grained upper tidal flats are known to be the best habitat for algal mats. They are detectable in multi-spectral optical images, but reflectance from them is low compared with that from chlorophyll in land. To distinguish such weak differences in reflectance, LSU method is supposed to be effective. Objective of this study is a classification of intertidal zone and detection of algal mats by applying LSU to Landsat ETM+ images. Determination of an effective end-member selection specifically in tidal flats was also conducted. Test site was the Saemangeum tidal flat in which three different sub-areas were studied. The calculated LSU components were used to review habitual characteristics of algal mat in terms of grain size and topography.

2. Test Site and Data

1) Saemangeum Tidal Flat

The Saemanguem tidal flat is located at the estuary of Mankyung and Donjin rivers discharging fresh water in the west coast of Korean Peninsula. The "Saemanguem Estuary" is bordered by Bian-Do in the north, Byunsan-Beach in the south and Gogunsan-Gundo in the west (Koh, 2001). A 30 km dike has been under construction since early 1990, and about 40,100 ha shallow estuary has been reclaimed.

Tides are semidiurnal with a mean tidal range of 430 cm (603 cm mean spring tide and, 276 cm mean neap tide) (Chun, 2002). Small intertidal channels and creeks are distributed in the tidal flat. The surface topography is relatively smooth and flat, and slope increases in the lower tidal flat (Lee and Kim, 1987). Three typical sub-areas are selected for this study including Kunsan, Kimje and Buan tidal flats which are divided by Mankyung and Dongjin rivers as in Figure 1.

2) Field and Satellite Data

Algal mats are usually observed in early spring when microphytobenthos bloom creates patches on the tidal flats. Field samples have been collected during five field surveys conducted between March 2002 and March 2003. In the field surveys, samples for spectral reflectance by a field spectrometer along with chlorophyll-a, grain size and water content have been measured. A differential GPS with a beacon

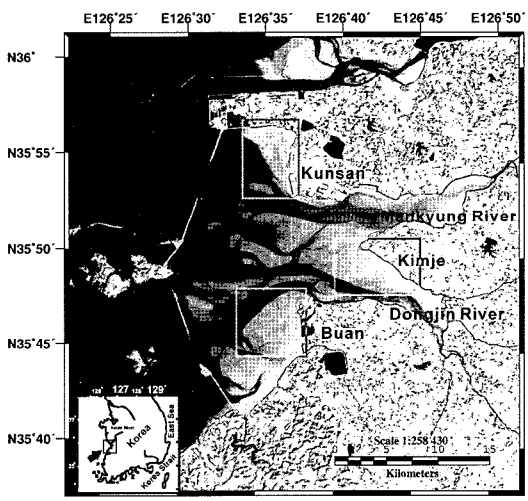

Fig. 1. Landsat ETM+ band 4 image of Saemangeum Estuary. The study area is divided into three areas (Kunsan, Kimje and Buan tidal flats) by Mankyung and Donjin Rivers for detailed investigation.

(Sokkia, AXIS 3) having a 1-m horizontal accuracy was used for precisely locating each sampling site.

The satellite data and the field data were collected on the same dates so as to maintain correlation between them but it was not possible because of weather and tidal conditions. Landsat ETM+ data acquired on 14 February 2002 were analyzed. Geometric rectification was conducted using IRS-1C Panchromatic satellite image which was rectified using topographic maps of 1:5,000 and 1:25,000 scales. A geometric accuracy within 0.3 pixels was achieved after geometric rectification. The COST model (Chavez, 1996) was used to correct atmospheric effects. The results of the COST model were effective in this study area and verified by comparison with 6S model (Na, 2003).

To examine the correlations between the satellite image and environmental factors including grain size, water content, spectral reflectance and algal mat, pixels in ETM+ image were determined to sampling locations. Samples for grain size analysis were collected from the top 1 cm of the surface sediments where they were not covered with water within a 1 m radius. After removing carbonate and organic materials, the grain size was measured its each sectional percentage using a Malvern Mastersizer Model 2000 which divided the particle size by grain size criteria of 0.0625 mm, 0.125 mm, 0.25 mm and 0.5 mm. Samples for water content measurement were obtained at the same points. MB45 (Ohaus Co.)was used for measuring water content. Reflectances in tidal flats were measured 5 times at the same place using FieldSpec FR (ASD Co.). Observing time was limited from 11 a.m. to 2 p.m. because reflectance of substance changes according to solar irradiance. The field spectrometer recorded reflectance data in the range from 350 nm to 2500 nm at an interval of 1 nm. A tripod was installed 1 m above the surface, 1519.79 cm^2 was measured at each site in sand and mud flats. When we measured algal mat, the sensor was positioned 15 cm above the surface with 34.73 cm^2 measured area in order to measure algal mat only within a heterogeneous tidal flat surface. Chlorophyll-a content was considered as algal mat content. Samples were collected using 14 mm syringe, then the samples were analyzed at 630 nm, 647 nm and 664 nm by absorbance measuring instrument (Pharmacia Biotech Co., Ultraspec 2000). To compare between spectrometer data, remote sensed image and chlorophyll-a content data, Jeffery and Humphrey (Jeffery and Humphrey, 1975) equation was applied to calculate chlorophyll-a content. Phopigment and chlorophyll-a showed the same optical characteristics.

3. Linear Spectral Unmixing (LSU)

1) Background

Measured optical spectra are supposed as a spectral sum of each pure end-member within a pixel. Each end-member has to represent spectra of pure land cover, and end-member selection have to be adjusted according to the physical characteristics of target area and object of the application (Lee and Lee, 2004). When a number of end-members is N, each end-member is located at each apex of N-dimensional polyhedron. Three end-members are in the each apex of triangle in the ideal case, the inner part of triangle is mixture space summed of end-members (Tso and Mather, 2001). Mathematically, Linear spectral unmixing (LSU) can be expressed as

$$R_b = \sum_{i=1}^{N} f_i R_{i,b} + e_b, \qquad (1)$$

when it is composed of N end-members. $R_{i,b}$ is an end-member to decompose the mixed reflectance spectra of each pixel, f_i the fraction of each end-

members, and e_b error. The sum of the fractions f_i should be 1 given by

$$\sum_{i=1}^{N} f_i = 1 , \qquad (2)$$

The error fraction e_b can be calculated from the difference of modeled (R_{jk}) and measured (R'_{jk}) digital number in band i. And n is the number of spectral bands and m is the number of pixels within the image. In generally, goodness of fit of model can be evaluated by error (e_b) or root mean squared (RMS) error. RMS error is calculated by equation (3).

$$RMS = \sum_{k=1}^{m} \frac{1}{m} \sqrt{\sum_{j=1}^{n} (R_{jk} - R'_{jk})^2 \Big/ n}, \qquad (3)$$

The error must be close to zero and not show any structure.

There are two types of end-member selections for LSU. The first method is based upon spectral library built from field or laboratory data, called 'reference end-member'. From the reference end-members, one can establish pure spectra through the field work, and it is easy to increase confidence level. However, reference end-members vary according to study areas due to locality of surface characteristics. The second method is to derive end-members from the satellite image itself that is called 'image end-member'. In this case, the selected pixel must represent pure end-member nature, ideally that is not mixed with other end-members (Asner and Heiderbrecht, 2002). The end-member selection methods are very important because the result of LSU is different according to the pixels selected as end-members. There are several methods for selecting 'image end-member', including 2D scattering analysis, principal component analysis (PCA), minimum noise fraction transformation (MNF), and pixel purity index (PPI).

2) Application of LSU

Figure 2 displays processing flow of this study. For

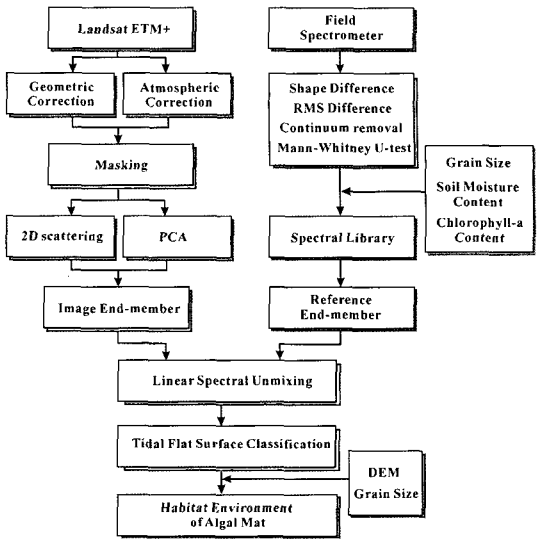

Fig. 2. Flow chart of this study.

reference end-members, we build a spectral library by applying RMS-difference of spectra, shape difference of spectra, continuum removal, and Mann-Whitney U-test to the field measured spectral data. Information of grain size, water content, chlorophyll-a content were also used in this step as in Figure 2. Image end-members were also selected from PCA-transformed satellite image that was atmospherically corrected. Land areas on the satellite image were masked out. Both reference and image end-members were used for comparison. We reviewed the relationship between algal mat fraction of the calculated LSU and *in-situ* measured chlorophyll-a content. The algal mat fractions were compared with chlorophyll-a content and Normalized Differenced Vegetation Index (NDVI). From the comparison, an effective end-member selection scheme in tidal flats was determined.

(1) Reference End-Member

Eighty two field spectra were obtained between April 2002 and March 2003. We selected typical spectra by RMS-difference and shape difference of spectra, continuum removal, and Mann-Whitney U-

test. Grain size, water content, chlorophyll-a content were used as auxiliary data to build a resulting spectral library. Spectral range from 450 nm to 900 nm was used for the spectral library as in Figure 3. After continuum removal, spectral characteristics of sand, mud, and algal mat show different patterns as in Figure 3(a). Reflectance from sand was generally higher than that from mud in the range from 550 nm to 900 nm in Figure 3(b). Algal mat showed a typical chlorophyll spectrum in the range from 450 nm to 540 nm, from 610 nm to 690 nm, but reflectance at near infrared was weaker than land vegetation. Because it was difficult to access to deep clear seawater, we derived spectral pattern of water from the image. Water has a typical absorption at near infrared range. Figure 3(b) displays spectra used for reference end-members in this study.

Although sand and mud are distinctive with continuum removal, general spectral patterns without continuum removal were similar each other. It was hard to classify sand and mud in the Landsat ETM+ image because these are heterogeneously mixed with each other within a pixel. Mud was excluded from end-members because the Saemangeum tidal flat is composed mostly of very fine sand when it was classified by Boggs' (Boggs, 1995) distribution method. Sand, algal mat and sea water were used as reference end-members.

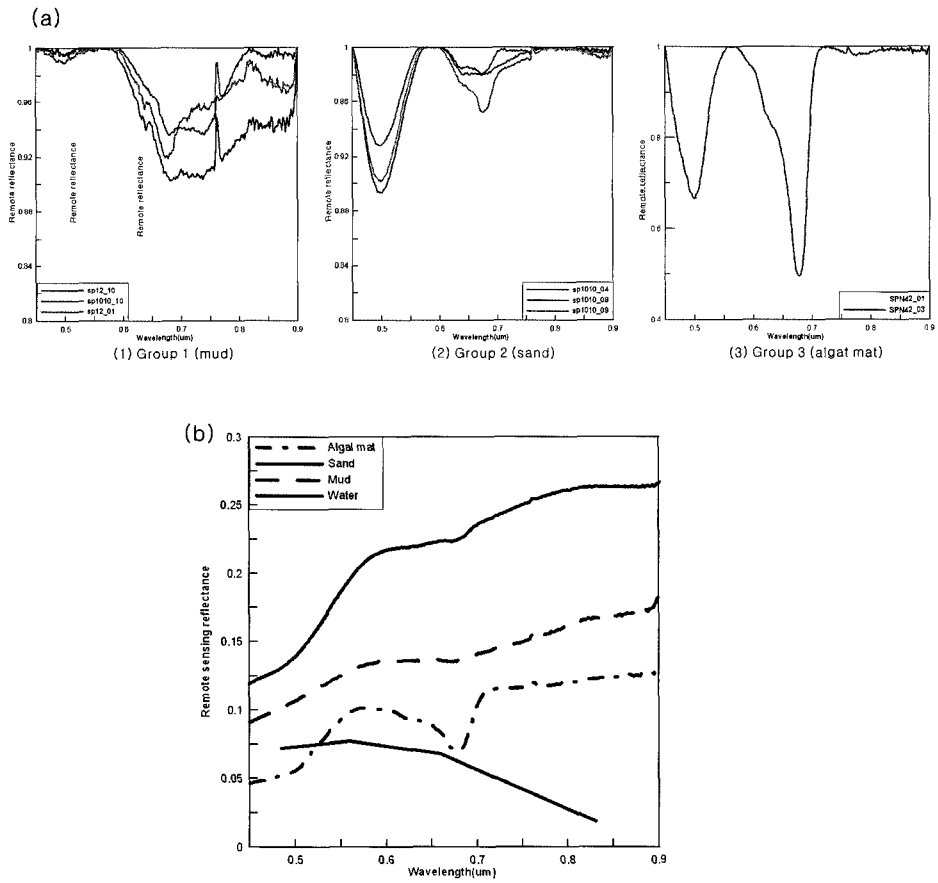

Fig. 3. (a) Spectral reflectance measured by field spectrometer after continuum removal, (b) reference end-members derived from RMS-difference, shape difference, continuum removal and Mann-Whitney U-test.

(2) Image End-Member

Image end-members were directly derived from the pixels representing pure end-members in the satellite image. The study area was subdivided into three sub areas including Kunsan, Kimje and Buan intertidal flats (Figure 1) which are separated by the Mankyung and Dongjin Rivers. 2-D scattering analysis was not effective to derive end-members in the study area. PCA transform showed good result to derive end-members as in Figure 4. Ideally, all pixels exist inside the mixture space (ie. triangle) which each end-member is located at the apex of the triangle. Pixels existed outside the mixture space cannot be represented by the selected end-members (Boardman, 1993). In such case, a nonlinear spectral unmixing must be used when many pixels locate outside the triangle (Small, 2001). End-members can, however, be selected from slightly outer or inner points from the extremities of the scatter plot because all pixels are hard to limited by end-members in the satellite image (Wu and Murray, 2003).

More than 90% of dispersion of Buan intertidal flats is on the principal component 1 (PC1) and 2 (PC2). Thus we used the PC1 and PC2 for the scatter plot in Figure 4. The selected end-members in the satellite image were confirmed by satellite image and field investigation. In the Buan tidal flats, a maximum of 4 end-members can be selected as in the Figure 4(b) in which marine aquaculture might be the fourth component. The marine aquaculture was excluded in our LSU because it is not the target of interest. Sediments, algal mat and water were selected end-members from the image, similar to reference end-members. In the Kimje tidal flats, the marine aquaculture sites were not seen as in Figure 4(c). End-members of Kunsan intertidal flats are shown in Figure 4(d). Due to sand shoal developed in Kunsan intertidal area, sediment end-member showed a distinctive feature compared with other sub areas.

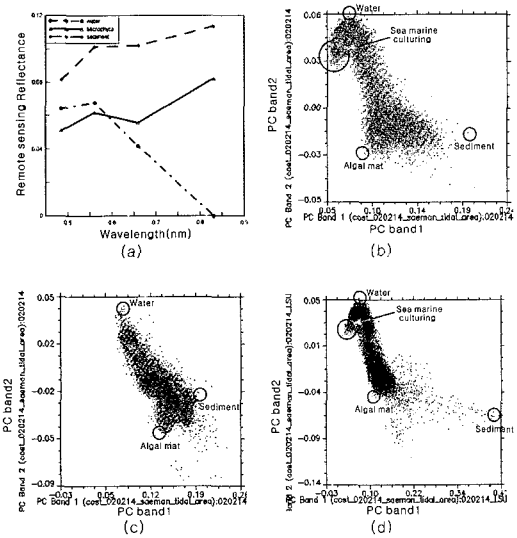

Fig. 4. Image end-members selected from PCA. (a) Reflectance of end-members derived from Buan tidal flats. Image end-members on the scatter plots of Buan (b), Kimje (c) and Kunsan (d).

4. Results and Discussion

1) Results of Linear Spectral Unmixing

Considering the wavelength of the reference end-member, Landsat ETM+ bands 1-4 were used for LSU calculation. Figure 5 is the LSU calculation by using both the reference and image end-members. The resulting images show three end-member fractions and an error fraction image in Figure 5. Dark areas in the LSU image present low density of the corresponding end-member fraction, while bright features are concentration of the end-member component. In all three Buan, Kimjae and Kunsan tidal flats, algal mat is well detected as bright features in the algal mat fraction or dark in the sediment fraction. The surface characteristics of the study area are represented by heterogeneous and complicated nature in terms of the three end-members. Sediment,

algal mat and water are mixed in the intertidal flats, it is difficult to find areas composed of a single end-member. Especially, microphytobenthos exist everywhere in tidal flats, but chlorophyll-a developed as patches in the uppermost sediment surface is better be detected and estimated by image (Riethmuller *et al.*, 2000). The results in Figure 5 demonstrate that LSU is an effective tool for detection of algal mat. Both the reference and image end-members succeeded in classifying algal mat fractions in the Kunsan, Kimje and Buan intertidal flats. The reference end-members were slightly better image algal mat in sediment and algal mat fraction in comparison with the results from image end-members. However, the reference end-members produced a systematic error fraction. The discernable structures in the error fraction imply that the errors are not random. It is considered that locally measured spectral data do not represent surface spectral characteristics of the entire area. No significant features are supposed to be found in error fraction, and image end-members were more effective than the reference end-members in terms of error fraction. Algal mat is well detected in the results from image end-members, but algal mat residing in small scale is not clearly detectable. Sand shoal developed in the Kunsan tidal flats was a distinctive feature and well imaged in ETM+ image, but less sensitive to sediment fraction of LSU. In the Buan intertidal flats, strong chlorophyll features are detected at lower tidal flats. Sea water front and intertidal channels are well separated from exposed bottom sediments specifically in the Buan and Kunsan tidal flats. Water fraction was effective to discriminate marine aquaculture structures appearing as dark squares in the Buan and Kunsan intertidal zones. In summary, LSU is very effective to detect algal mat and water body from bottom sediments especially if reference end-members are used but less sensitive to sediment types.

The accuracy of LSU can be evaluated by comparing the estimated values with ground truth data. Algal mat fractions were compared with chlorophyll-a content. Field observations had been

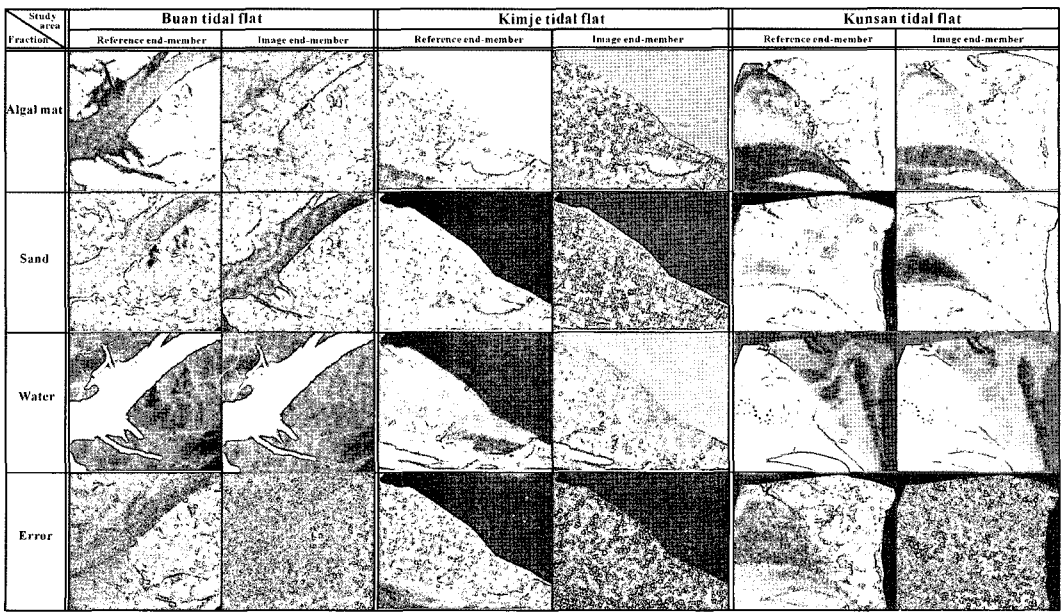

Fig. 5. The results of linear spectral unmixing. Algal mat is rendered by bright features in the algal mat fraction and dark in the sediment fraction.

carried out on 19 April 2002 and 18 February 2003 in the Buan intertidal zone, 19 February 2003 in the Kimje intertidal zone, and 20 February and 4 March 2003 for Kunsan intertidal zone. The correlation coefficients between algal fractions and *in-situ* sampled chlorophyll-a content were very poor as in Table 2 except in the Kunsan intertidal area. These results can be explained by the facts: i) field surveys and satellite data acquisition did not coincide; ii) chlorophyll-a data do not represent LSU reflectance because of difference of spatial resolution between satellite image and field observation; iii) optical reflectance from microphytobenthos largely varies according to exposure time while our *in-situ* chlorophyll-a content presents a total amount above and below the surface; and iv) Landsat ETM+ which has relatively low spectral resolution. In fact, it is still an open question whether satellite remote sensing is able to quantitatively estimate the amount of algal mat or not. It is because algal mat stays below surface under seawater and begins to come out above the surface when the surface is exposed to the air while remote sensing is only possible to observe it when it exposes to the air. Based upon the results in Table 2 and tidal and topographic conditions, we reached to a conclusion that the algal mat in the Kunsan tidal flats had been exposed enough time to the air when the Landsat data was acquired. NDVI is very sensitive to algal mat, and the calculated algal mat fraction images were correlated with NDVI. If algal mat fraction is positively correlated with the NDVI, then one can presume that the chlorophyll fractions derived by LSU are reasonably correct. Table 3 is the correlation coefficients of the estimated algal mat fractions and NDVI. The correlation coefficient R between the results from reference end-members and NDVI was 0.80~0.86, and those from image end-member and NDVI was 0.78~0.79. End-members from spectral library performed slightly better than image end-members. Although it was not possible to quantitatively measure algal mat density, LSU proves to be useful for accurately determining algal mat in tidal flats. It would be necessary to utilize hyperspectral approach in the follow-up researches.

Table 1. Summary of *in situ* data.

Field survey dates	Class and number of samples	
2002.03.31 ~ 2002.04.03	Grain size	285
2002.04.18 ~ 2002.04.19	Soil moisture	92
2002.04.18 ~ 2002.04.19	Spectrometer	82
2003.02.15 ~ 2003.02.20	Chlorophyll-a	116
2003.03.03 ~ 2003.03.07		

Table 2. The correlation coefficient of algal mat fraction with chlorophyll-a content for each study area.

	Reference end-member	Image end-member
Buan	-0.10	-0.24
Kimje	-0.12	-0.23
Kunsan	0.57	0.58

Table 3. The correlation coefficient of algal mat fraction with NDVI for each study area.

	Reference end-member	Image end-member
Buan	0.82	0.78
Kimje	0.86	0.79
Kunsan	0.80	0.79

2) Habitat of Algal Mat

We investigated habitat of the detected algal mat with respect to grain size and tidal flat location. Fine grained upper tidal flats are generally considered as a typical habitat of microphytobenthos, especially micro-benthic diatom. In other field surveys showed high density of microphytobenthos in the upper tidal flats of Mankyung and Dongjin Rivers and low density in the lower tidal flat near small channels (Oh and Koh, 1995). After the tidal flat bottom surface is exposed to air, algal mat begins to emerge from below the surface. Microphytobenthos prefer longer exposure time to the Sun. Upper tidal flat has longer exposure time with low

tidal energy and the best conditions for most microphytobenthos. The common characters of algal mat patches are the place highly effected by sea water input and output, and these are near channels. It is considered that diatom, main species of algal mat, resides on the place where sea water is often mixed by wind (Barnes and Manns, 2002).

In Figure 6, we plotted the detected algal mats from LSU images onto tidal flat DEMs. In the Kunsan tidal flats (Figure 6(a)), algal mat spread out from upper to lower tidal flats. In the Kimje tidal flats Figure 6(b), algal mat thrives on mud bank about one or two meters higher than surroundings. Algal mats developed on the lower tidal flat in the Buan tidal flats as in Figure 6(c) . The algal mat patches detected in this study in the lower tidal flats were verified by field works in February 2002. As discussed before, it is very unusual to find microphytobenthos blooming in the lower tidal flats. Now let us consider grain size of the algal mat habitat. Algal mat normally thrives in fine grained upper tidal flats. However, the algal mats that we detected showed quite different habitat from a generally known one. Algal mat patches that we found from LSU locate lower tidal flats as well as expected upper tidal flats.

Figure 7 displays that mud and very fine sand (i.e. fine-grained sediments) are dominant in the Kunsan and Kimje tidal flats. However, grain size in Buan lower tidal flats is dominated by fine sand (i.e. coarse-grained sediments). Existence of the algal mat patches on the fine sand were confirmed by field work in

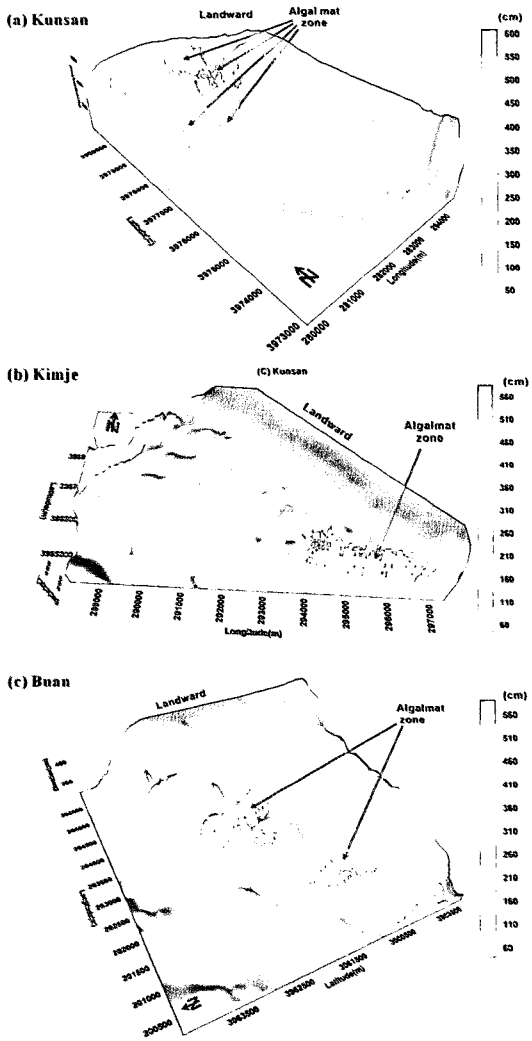

Fig. 6. DEM overlaid with detected algal mat patches from the LSU algal mat fraction.

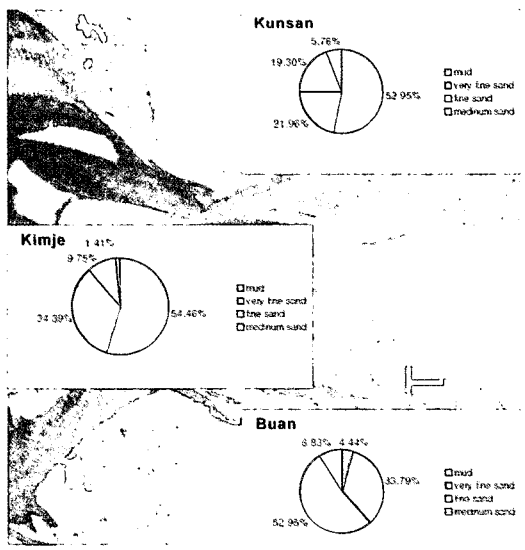

Fig. 7. The measured grain size at the detected algal mat patches. Note that algal mat habitat in the Buan tidal flats is dominated by fine sand.

February 2002. In conclusion, the algal mat in the Buan tidal flats detected by LSU in this study showed uncommon habitat that is fine-grained lower tidal flats.

5. Conclusions

A linear spectral unmixing using Landsat ETM+ images was very effective to detect algal mat in the Saemangeum tidal flats. End-members were selected from both spectral library and image itself. LSU results showed that the classified layer of algal mat is relatively well correlated with NDVI image. Reference end-members from the spectral library were slightly more effective than that of image end-member for discriminating algal mat from sediments. Image-end members were superior to reference end-members in terms of error fraction. It was not possible to do volumetric estimation of algal mat in tidal flats by remotely sensed data alone.

Algal mat in the Saemangeum tidal flats was detected on the coarse-grained lower tidal flat as well as on the fine-grained upper tidal flats. Fine sediments in Kunsan and Kimje upper tidal flats provide a rich habitat for algal mat. However, uncommon algal mat habitat was found in the Buan tidal flats that were characterized by unexpected environment, lower tidal flats with coarse sediment compositions. From a review of time sequenced Landsat images, algal mat was not found at the same areas until early 1990's. The microphythobenthos began to exist since Saemangeum dike construction in 1991. We do not know the environmental factors triggering the algal mat emergence in this specific area. This algal mat must be continuously monitored by high resolution satellite such as KOMPSAT-2 or hyperspectral sensors.

To understand the algal mat thriving in the Buan lower tidal flats, high resolution multi-spectral image is necessary to delineate the boundary of algal mat in the blooming season from January to early March. Environmental effects of the dike construction should also need to quest in the future studies. To achieve the final goals, remote sensing specialists and biologists must work together in this areas.

Acknowledgment

This work was supported by the Korea Ministry of Science under a grant of Space Development Program.

References

Asner, G. P. and K. B. Heiderbrecht, 2002. Spectral unmixing of vegetation, soil and dry carbon cover in arid regions: comparing multispectral and hyperspectral observations, *International Journal of Remote Sensing*, 23(19): 3939-3958.

Barnes, R. S. K. and K. H. Manns, 2002. *Fundamental of aquatic geology*, Acanet.

Boardman, J. W., 1993. Automating spectral unmixing of AVIRIS data using convex geometry concepts. *Proceedings of the Airborne Visible/Infrared Imaging Spectrometer (AVIRIS)*, Airborne Geoscience Workshop. JPL, Jet Propulsion Laboratory, Pasadena, USA, pp. 11-14.

Boggs, S. J., 1995. *Principles of Sedimentology and Stratigraphy*, Prentice Hall.

Chavez, P. S., Jr., 1996. Image-Based Atmospheric Corrections-Revisited and Improved, *Photogrammetric Engineering & Remote Sensing*, 62(9): 1025-1036.

Chun, S. S., 2002. *Physical Environment of*

Saemangeum Estuary (Korean ed.). The Korean Society for the Life of Saemangeum, pp. 26-31.

Koh, C. H., 2001. *The Korean tidal flat: environment, biology and human (Korean ed.)*, Seoul National University Press.

Lee, C. B. and T. Kim, 1987. Formation and evolution of turbidity maximum in the Keum Estuary, west coast of Korea, *The Journal of the Oceanological Society of Korea*, 9: 293-307.

Lee, J. M. and K. S. Lee, 2004. Analysis of forest cover information extracted by spectral mixture analysis, *Korean Journal of Remote Sensing*, 19(6): 411-419.

Na, Y. H., 2003. *A study on surface change and optical reflectance of the Saemangeum tidal flat by remote sensing (Korean ed.)*. M.S. Thesis, Yonsei Univeristy.

Oh, S. H. and C. H. Koh, 1995. Distribution of diatoms in the surfacial sediments of the Mankyung-Dongjin tidal flat, west coast of KOREA(Eastern Yellow Sea), *Marine Biology*, 122: 487-496.

Paterson, D. M. *et al.*, 1998. Microbiological mediation of spectral reflectance from interidal cohesive sediments, *Limnology and Oceanography*, 43: 1207-1221.

Riethmuller, R., M. Heineke, H. Kuehl, and R. Keuker-Ruediger, 2000. Chlorophyll a concentration as an index of sediment surface stabilization by microphytobenthos?, *Continental Shelf Research*, 20: 1351-1372.

Roberts, D. A. *et al.*, 1998. Mapping chaparral in the Santa Monica mountains using multiple endmember spectral mixture models, *Remote Sensing of Environment*, 65: 267-279.

Small, C., 2001. Estimation of urban vegetation abundance by spectral mixture analysis, *International Journal of Remote Sensing*, 22(7): 1305-1334.

Tso, B. and P. M. Mather, 2001. *Classification Methods for Remotely Sensed Data*, Taylor & Francis.

Wu, C. and A. T. Murray, 2003. Estimating impervious surface distribution by spectral mixture analysis, *Remote Sensing of Environment*, 84: 493-505.